Superparamagnetic iron oxide nanoparticles enhance glioma radiosensitivity via inducing cell cycle arrest and apoptosis

Jinning Mao
second affiliated hospital of Chongqing Medical University
Meng Jiang
Suzhou University: Soochow University
Xingliang Dai
Anhui Medical University
Guodong Liu (304678@hospital.cqmu.edu.cn)
second affiliated hospital of Chongqing Medical University https://orcid.org/0000-0002-8048-2243
Zhixiang Zhuang
Suzhou University: Soochow University
Jun Dong
Suzhou University: Soochow University

Research article

Keywords: Superparamagnetic iron oxide nanoparticles, glioma, radiosensitivity, cell cycle

Posted Date: October 26th, 2020

DOI: https://doi.org/10.21203/rs.3.rs-93279/v1

Abstract

Aim: Superparamagnetic iron oxide nanoparticles (SPIONs) is a widely used biomedical material for imaging and targeting drug delivery. We synthesized SPIONs and tested their effects on the radiosensitization of glioma.

Methods: Acetylated 3-aminopropyltrimethoxysilane (APTS)-coated iron oxide nanoparticles (Fe_3O_4 NPs) were synthesized via a one-step hydrothermal approach and the surface was chemically modified with acetic anhydride to generate surface charge-neutralized NPs. NPs were characterized by TEM and ICP-AES. Radiosensitivity of U87MG glioma cells was evaluated by MTT assay. Cell cycle and apoptosis in glioma cells were examined by flow cytometry.

Results: APTS-coated Fe_3O_4 NPs had a spherical or quasi-spherical shape with average size of 10.5±1.1 nm. NPs had excellent biocompatibility and intracellular uptake of NPs reached the peak 24 hours after treatment. U87 cell viability decreased significantly after treatment with both X-ray and NPs compared to X-ray treatment alone. Compared to X-ray treatment alone, the percentage of cells in G2/M phase (31.83%) significantly increased in APTS-coated Fe_3O_4 NPs plus X-ray treated group ($P<0.05$). In addition, the percentage of apoptotic cells was significant higher in APTS-coated Fe_3O_4 NPs plus X-ray treated group than in X-ray treatment alone group ($P<0.05$).

Conclusion: APTS-coated Fe_3O_4 NPs achieved excellent biocompatibility and increased radiosensitivity for glioma cells.

Introduction

Glioma is the most common malignant primary brain tumor in the adults and occurs about five cases per 100,000 population per year [1,2,3]. Despite the advances in surgery therapy, radiotherapy and chemotherapy, the prognosis of glioma is still poor, and glioma recurs in most patients within 1 to 5 year[4,5]. Radiotherapy (RT) could penetrate into tissues deeply and it is important to improve radiation delivery technology to minimize its secondary damage to the surrounding normal tissues[6,7]. The side effects of RT such as granulocytopenia or radiation encephalopathy cause trouble to many patients[8,9]. Therefore, many nanoparticles such as water-soluble carbon nanotubes, fullerene-C60, silver and golden nanoparticle have been developed to decrease the side effects, and at the same time, radiosensitivity is increased [10–14].

Radiosensitization of high atomic number (Z) metallic nanoparticles such as golden nanoparticle and sliver nanoparticle has been reported. X-ray beams with high energies in the presence of high-atomic number nanoparticles lead to not only secondary electrons including auger electrons but also high-energy electrons produced by coulomb interaction of electron and nuclei field. Either electrons or photons disperse in the target volume and their absorption will increase in the presence of high-Z metallic nanoparticles, eventually killing tumor cells. Superparamagnetic iron oxide nanoparticles (SPIONs) as a

kind of high-Z nanoparticle have attracted broad interest and intense attention because of the potential as contrast agents for magnetic resonance imaging (MRI) and other biomedical applications such as multimodal biomedical imaging and targeting drug delivery[15,16]. SPIONs are mono-crystalline nanoparticles with properties of superparamagnetism and biocompatibility [17,18,19]. Superparamagnetism could guide SPIONs to the targeting area through an external autoclaved inhomogeneous magnetic field. In addition, biocompatibility and effective biodistribution of SPIONs allow for their broad medical application[20]. In this study, we aimed to develop SPIONs for glioma radiotherapy. We synthesized SPIONs and tested their effects on the radiosensitization of glioma.

Materials And Methods

NPs synthesis

3-aminopropyltrimethoxysilane (APTS) coated Fe_3O_4 NPs were synthesized using hydrothermal approach as described previously[21]. Briefly, 1 g $FeCl_2{\cdot}4H_2O$ was dissolved in 6.2 ml distilled water, then 5 ml ammonium hydroxide was added and the suspension was continuously stirred at room temperature for 10 min. Then, 2 ml APTS was added and the mixture was autoclaved at 134℃ for 3 h. Then the mixture was cooled and purified with distilled water, then centrifuged (5,000 rpm, 10 min) to remove excess reactants. The process was repeated for five times to get APTS-coated Fe_3O_4 NPs.

The amine groups were connected on the surface of APTS-coated Fe_3O_4 NPs via a reaction with acetic anhydride. In brief, 6 mg APTS-coated Fe_3O_4 NPs was dispersed in 5 ml ethanol and mixed with 1 ml of triethylamine. 5 ml dimethyl sulfoxide (DMSO) containing 1 ml acetic anhydride was then added and mixed for 24 h. Then the mixture was purified with distilled water, then centrifuged to remove excess reactants. The process was repeated for three times to get acetylated APTS-coated Fe_3O_4 NPs.

Characterization of NPs

The morphology of NPs was observed under JEO2010 F transmission electron microscope (Akishima-shi, Japan) operated at 200 kV. The size of NPs was measured using Image J image analysis software. The size distribution histogram was obtained via different TEM images. Fe concentration of APTS-coated Fe_3O_4 NPs was tested with Prodigy inductively coupled plasma-atomic emission spectroscopy (ICP-AES) (PerkinElmer Optima 8000, USA).

The intracellular uptake of NPs

The intracellular uptake of APTS-coated Fe_3O_4 NPs was quantified via ICP-AES analysis with Prodigy ICP-AES system (PerkinElmer Optima 8000, USA). U87 cells were seeded in six-well plates at density of 1×10^6 per well and cultured for 24 h, then incubated with different concentrations of acetylated APTS-coated Fe_3O_4 NPs (0, 10, 25, 50, and 100 μg/ml) for 24 h or incubated with 25 μg/ml acetylated APTS-coated Fe_3O_4 NPs for 6, 12, 24, 48 or 72 h. The culture medium was removed and the cells were washed with

PBS three times. The cells were collected and lysed. The amount of iron in the lysates was quantified with ICP-AES.

MTT assay

The viability of U87 glioma cells was tested via MTT assay as described previously[22]. Briefly, U87 cells were seeded into a 96-well plate with 1×10^4 per well and incubated for 24 h. Next the cells were incubated with different concentrations of acetylated APTS-coated Fe_3O_4 NPs (0, 1, 10, 20, 40, and 80 μg/ml) for another 24 h, then treated with or without irradiated with different dose of X-ray (0,2,4,6,8,10 Gy) and cultured for 24 h. 20 μl of 5 mg/ml MTT solution was added to each well. After 4 h of incubation, the medium was removed and 200 μl DMSO was added. The absorbance was measured in a BioTek Elx800 (Thermo Scientific, Waltham, MA, USA) at a wavelength of 490 nm. The inhibition of cell growth was calculated with following formula: Cell viability (%) = (mean of Abs. value of treatment group/mean of Abs. value of control group)×100%. All treatments were carried out in triplicate.

Apoptosis assay

Apoptotic cells were detected by double-staining with annexin V-fluorescein isothiocyanate (FITC) and propidium iodide (PI). U87 cells were treated with APTS-coated Fe_3O_4 NPs or/and X-rays as described above. The cells were collected and resuspended in Annexin V binding buffer, then stained by Annexin V-FITC and PI according to the protocol of Annexin V-FITC Apoptosis Detection Kit (Sigma). Analysis of stained cells was performed in triplicate with each sample of 20,000 cells by a FACSCalibur flow cytometer (Becton–Dickinson, BD Biosciences, Ontario, Canada).

Cell cycle analysis

U87 cells were treated with APTS-coated Fe_3O_4 NPs or/and X-rays as described above. The cells were collected and resuspended in DNA staining solution (Multiscience, China) containing 10 μg/ml RNase and 50 μg/ml PI, then stained by PI for 30 min at room temperature in the dark. Analysis of stained cells was performed in triplicate with each sample of 20,000 cells by a FACSCalibur flow cytometer (Becton–Dickinson, BD Biosciences, Ontario, Canada). The data were analyzed by ModFit LT software.

Statistical analysis

Values were expressed as the mean ± standard deviation (SD) and analyzed by SPSS version 13.0. Statistical analysis was carried out using t test or χ^2 test. $P<0.05$ was considered significant.

Results

Characterization of APTS-coated Fe_3O_4 NPs

The acetylated APTS-coated Fe_3O_4 NPs were synthesized, and then were characterized by TEM. TEM images indicated that the particles had a spherical or quasi-spherical shape (Fig. 1A). The size distribution of APTS-coated Fe_3O_4 NPs characterized by TEM was shown in Fig. 1B. The average size of APTS-coated Fe_3O_4 NPs was 9.8±1.1 nm (Fig. 1B). In addition, DLS technique was employed to show that dominant fraction of NP diameter was about 13 nm (Fig. 1C). The average particle sizes determined by TEM and DLS were consistent.

The intracellular uptake of NPs

ICP-AES analysis showed that intracellular iron content increased in U87 cells with increased concentration of acetylated APTS-coated Fe_3O_4 NPs in culture medium (Fig. 2A). In addition, intracellular iron content increased with the prolongation of treatment time and reached peak at 24 h after treatment with acetylated APTS-coated Fe_3O_4 NPs, and then gradually decreased over time (Fig. 2B). Therefore, in the following experiments 24 h was selected as the appropriate time point.

NPs increased glioma cell radiosensitivity

MTT assay showed that different concentrations of acetylated APTS-coated Fe_3O_4 NPs had minimal effects on the growth of U87 cells (Fig. 3A). These results indicated good biocompatibility of NPs. On the other hand, X-ray decreased U87 cell viability in a dose dependent manner (Fig. 3B). 4 Gy X-ray inhibited cell viability by about 25%, and was used in the following experiments. As shown in Fig. 3C, cell viability decreased significantly in cells treated with both X-ray and NPs compared to cells treated with X-ray alone. These data indicated that NPs increased glioma cell radiosensitivity.

NPs promoted radiation induced G2/M phase arrest of glioma cells

To understand how NPs increased glioma cell radiosensitivity, we examined cell cycle profiles of U87 cells treated with 20 μg/ml APTS-coated Fe_3O_4 NPs or/and irradiation. While 19.54% of cells were in G2/M phase in untreated control group, 15.84% of cells were in G2/M phase in APTS-coated Fe_3O_4 NPs treated group, showing no significant difference. However, compared to the percentage of cells in G2/M phase in X-ray treatment alone (25.51%), there was a significant increase in the percentage of cells in G2/M phase (31.83%) in APTS-coated Fe_3O_4 NPs plus irradiation treated group ($P<0.05$, Fig. 4). These results indicated that NPs promoted radiation induced G2/M phase arrest of glioma cells.

NPs promoted radiation induced apoptosis of glioma cells

Furthermore, we examined apoptosis of U87 cells treated with 20 μg/ml APTS-coated Fe_3O_4 NPs or/and irradiation. As shown in Fig. 5, AnnexinV+/PI- (lower right quadrant, LR) cells underwent early apoptosis with intact membranes while Annexin V+/PI+ (upper right quadrant, UR) cells were in the final stage of apoptosis. Quantitate analysis showed that the percentage of apoptotic cells (LR+UR) was significant higher in irradiation treated group than in untreated group, and was significant higher in APTS-coated

Fe_3O_4 NPs plus irradiation treated group than in irradiation alone treated group ($P<0.05$, Table 1). These results indicated that NPs promoted radiation induced apoptosis of glioma cells.

Discussion

The presence of macromolecules such as serum proteins may affect the stability of NPs and cause the agglomeration and sedimentation of NPs, impairing biological effects of NPs and even inducing side effects[19,20]. Therefore, it is important to establish compatible physiologically or chemical conditions to improve nanoparticle stability for biomedical applications. The amine groups on the surface of APTS-coated Fe_3O_4 NPs were further acetylated via a reaction with acetic anhydride, which endowed Fe_3O_4 NPs with an excellent water dispersibility and colloidal stability. Moreover, APTS-coated Fe_3O_4 NPs can be further functionalized with acetyl groups with neutral surface potential following the reaction of the surface APTS amines with acetic anhydride[21]. In present study, acetylated APTS coated Fe_3O_4 NPs with a mean diameter of 10.5 nm were synthesized, and APTS-coated Fe_3O_4 NPs in a powder form could be dissolved in water, PBS, or cell culture medium with good colloidal stability following storage at 4°C for at least 1 month without obvious precipitates.

TEM images showed that the mean diameter of NPs was 10.5 ± 1.1 nm, with a narrow distribution without obvious agglomeration. NPs with diameter in such range can be easily engulfed by cells as demonstrated in other studies[13,18,19]. In this study, cellular uptake of acetylated APTS-coated Fe_3O_4 NPs was quantified via ICP-AES, and iron uptake by glioma cells was concentration dependent. MTT assay showed that acetylated APTS-coated Fe_3O_4 NPs had no significant cytotoxicity to glioma cells, but increased the cytotoxicity of X-ray in glioma cells.

G0/G1 is the cell cycle phase that is most resistant to radiotherapy while G2/M is the phase that is most sensitive to radiotherapy[22,23]. To reveal the mechanism by which acetylated APTS-coated Fe_3O_4 NPs increased radiosensitivity of glioma cells, we examined cell cycle and apoptosis in different treatment groups. The results showed that G2/M ratio increased significantly and G0/G1 ratio decreased significantly in NPs and X-ray combined treatment group compared to NPs or X-ray alone treatment group. In addition, apoptosis ratio increased significantly in NPs and X-ray combined treatment group compared to NPs or X-ray alone treatment group. These data indicate that APTS-coated Fe_3O_4 NPs enhance radiosensitivity by promoting G2/M cell cycle arrest and enhancing apoptosis of glioma cells. Further *in vivo* experiments are needed to evaluate the potential of acetylated APTS-coated Fe_3O_4 NPs in radiotherapy.

In conclusion, we synthesized acetylated APTS-coated Fe_3O_4 NPs via hydrothermal approach and they had excellent bio-compatibility and chemical stability. Importantly, APTS-coated Fe_3O_4 NPs can increase cytotoxicity of X-ray through the regulation of cell cycle and apoptosis of glioma cells. These results provide evidence that APTS-coated Fe_3O_4 NPs are effective sensitizer for glioma radiotherapy.

Declarations

Acknowledgements

The radiosensitivity experiment was partly performed in the lab of Department of Radiotheraphy, The Second Affiliated Hospital of Chongqing Medical University.

Statement of Ethics

The research protocol was approved by the Research Ethics Committee of Chongqing Medical University, China.

Disclosure Statement

The authors declare no competing interests.

Funding Sources

This study was supported by National Nature Science Foundation of People's Republic of China (81401500), Science Foundation of Chongqing Municipality, People's Republic of China (cstc2019jcyj-msxmX0231), Science Foundation of Jiangsu Province, People's Republic of China (BK20140298). High-level Medical Reserved Personnel Training Project of Chongqing.

Author contributions

Jinning Mao &Meng Jiang contributed equally to this article. They synthesized the nanoparticles. Xingliang Dai &Zhixiang Zhuang conducted the *in vitro* experiments, Jun Dong conducted the *in vivo* experiments. Guodong Liu analysed the results. All authors reviewed the manuscript.

References

1. Metellus P, Coulibaly B, Colin C, de Paula AM, Vasiljevic A, Taieb D, Barlier A, Boisselier B, Mokhtari K, Wang XW, Loundou A, Chapon F, Pineau S, Ouafik L, Chinot O, Figarella-Branger. D.Absence of IDH mutation identifies a novel radiologic and molecular subtype of WHO grade II gliomas with dismal prognosis. *Acta Neuropathologica*.6, 719–729,doi: 10.1007/s00401-010-0777-8(2010).
2. Orringer D, Lau D, Khatri S, Zamora-Berridi GJ, Zhang K, Wu C, Chaudhary N, Sagher O. Extent of resection in patients with glioblastoma: limiting factors, perception of resectability, and effect on survival. J Neurosurg. 2012;5:851–9,. doi:10.3171/2012.8.
3. Gurusamy R, Subramaniam V. A Machine Learning Approach for MRI Brain Tumor Classification. CMC: Computers Materials Continua. 2017;2:91–108.
4. Tian H, Cong P, Qi R, Gao X, Liu X, Liu H, Shan F. Decreased invasion ability of hypotaurine synthesis deficient glioma cells was partially due to hypomethylation of Wnt5a promoter. Biocell. 2017;1:27–32.

5. Amichetti M, Amelio D. A Review of the Role of Re-Irradiation in Recurrent High-Grade Glioma (HGG). Cancers (Basel). 2011;4:4061–89,. doi:10.3390/cancers3044061.
6. Mamounas EP, Kuehn T, Rutgers EJT, &von Minckwitz G. Current approach of the axilla in patients with early-stage breast cancer. Lancet. 2017;17(17):31451–4. doi: 10.1016/S0140-6736).
7. Yang H, Lin Y, Liang Y. Treatment of Lung Carcinosarcoma and Other Rare Histologic Subtypes of Non-small Cell Lung Cancer. Current Treatment Options In Oncology. 2017;9:54. doi:10.1007/s11864-017-0494-9.
8. Álvarez-Camacho M, Gonella S, Campbell S, Scrimger RA, &Wismer WV. A systematic review of smell alterations after radiotherapy for head and neck cancer. *Cancer Treatment Reviews*, 54, 110–121, doi: 10.1016/j.ctrv.2017.02.003(2017).
9. Lipsett A, Barrett S, Haruna F, Mustian K, O'Donovan A. The impact of exercise during adjuvant radiotherapy for breast cancer on fatigue and quality of life: A systematic review and meta-analysis. *Breast*,32,144–155,doi: 10.1016/j.breast.2017.02.002(2017).
10. Jeyamohan P, Hasumura T, Nagaoka Y, Yoshida Y, Maekawa T, Kumar DS. Accelerated killing of cancer cells using a multifunctional single-walled carbon nanotube-based system for targeted drug delivery in combination with photothermal therapy. Int J Nanomed. 2013;8:2653–67,. doi:10.2147/IJN.S46054.
11. Ni J, Wu Q, Li Y, Guo Z, Tang G, Sun D, Gao F. &Cai, J. Cytotoxic and radiosensitizing effects of nano-C60 on tumor cells *in vitro*. J Nanopart Res. 2008;4:643–51.
12. Xie WZ, Friedland W, Li WB, Li CY, Oeh U, Qiu R, Li JL, Hoeschen C. Simulation on the molecular radiosensitization effect of gold nanoparticles in cells irradiated by x-rays. *Physics in Medicine and Biology*, 16, 6195–6212,doi: 10.1088/0031-9155/60/16/6195(2015).
13. Liu P, Huang Z, Chen Z, Xu R, Wu H, Zang F, Wang C, Gu N. Silver nanoparticles: a novel radiation sensitizer for glioma? *Nanoscale*.**23**, 11829–11836, doi: 10.1039/c3nr01351k(2013).
14. Chen-Sandoval J, Perry CC, Yun J, Chan PJ. HPV-associated cervical cancer cells targeted by triblock copolymer gold nanoparticle curcumin combination. Eur J Gynaecol Oncol. 2017;3:413–7.
15. Wahajuddin, Arora S. Superparamagnetic iron oxide nanoparticles: magnetic nanoplatforms as drug carriers. Int J Nanomed. 2012;7:3445–71,. doi:10.2147/IJN.S30320.
16. Alwi R, Telenkov S, Mandelis A, Leshuk T, Gu F, Oladepo S, Michaelian K. Silica-coated super paramagnetic iron oxide nanoparticles (SPION) as biocompatible contrast agent in biomedical photoacoustics. Biomedical Optics Express. 2012;10:2500–9. doi:10.1364/BOE.3.002500.
17. Lee CM, Jeong HJ, Kim SL, Kim EM, Kim DW, Lim ST, Jang KY, Jeong YY, Nah, JW&Sohn, MH. SPION-loaded chitosan–linoleic acid nanoparticles to target hepatocytes. *International Journal of Pharmaceutics*, **1–2**,163–169. doi: 10.1016/j.ijpharm.2008.12.021(2009).
18. Silva AH, Lima E, Jr, Mansilla MV, Zysler RD, Troiani H, Pisciotti MLM, Locatelli C, Benech JC, Oddone N, Zoldan VC, Winter E, Pasa AA, Creczynski-Pasa TB. Superparamagnetic iron-oxide nanoparticles mPEG350- and mPEG2000-coated: cell uptake and biocompatibility evaluation. *Nanomedicine*, 4, 909–919. doi: 10.1016/j.nano.2015.12.371(2016).

19. Hong GB, Zhou, JX&Yuan, RX. Folate-targeted polymeric micelles loaded with ultrasmall superparamagnetic iron oxide: combined small size and high MRI sensitivity. Int J Nanomed. 2012;7:2863–72. doi:10.2147/IJN.S25739.
20. Jin R, Lin B, Li D, &Ai H. Superparamagnetic iron oxide nanoparticles for MR imaging and therapy: design considerations and clinical applications. *Current Opinion in Pharmacology*, 18, 18–27, doi: 10.1016/j.coph.2014.08.002(2014).
21. Li K, Shen M, Zheng L, Zhao J, Quan Q, Shi X, Zhang G. Magnetic resonance imaging of glioma with novel APTS-coated superparamagnetic iron oxide nanoparticles. Nanoscale Res Lett. 2014;1:304. doi:10.1186/1556-276X-9-304(.
22. Wu J, Sun J. Investigation on mechanism of growth arrest induced by iron oxide nanoparticles in PC12 cells. J Nanosci Nanotechnol. 2011;12:11079–83. DOI:10.1166/jnn.2011.3948.
23. Yang C, He X, Chen J, Chen D, Liu Y, Xiong F, Shi F, Dou J, Gu N. Fe_3O_4 nanoparticle loaded paclitaxel induce multiple myeloma apoptosis by cell cycle arrest and increase cleavage of caspases *in vitro*. *Journal of Nanoparticle Research*, 15, 1840. DOI 10.1007/s11051-013-1840-x(2013).

Tables

Table 1. Apoptosis of U87 cells in different treatment groups.

	UL (%)	LL (%)	UR (%)	LR (%)	UR+LR (%)
Untreated	0.35±0.01	98.89±0.28	0.48±0.02	0.28±0.02	0.76
NPs treated	1.67±0.21	95.03±2.59	1.11±0.57	1.19±0.38	2.3
4 Gy treated	15.89±3.49	70.37±9.38	6.26±2.12	7.48±2.46	13.74*
NPs + 4Gy	10.75±2.53	67.82±8.65	12.39±3.49	9.04±1.98	21.43*,#

The value was presented as mean±SD (n=3). *Compared to untreated group, P<0.05; #Compared to 4 Gy treated group, P<0.05.

Figures

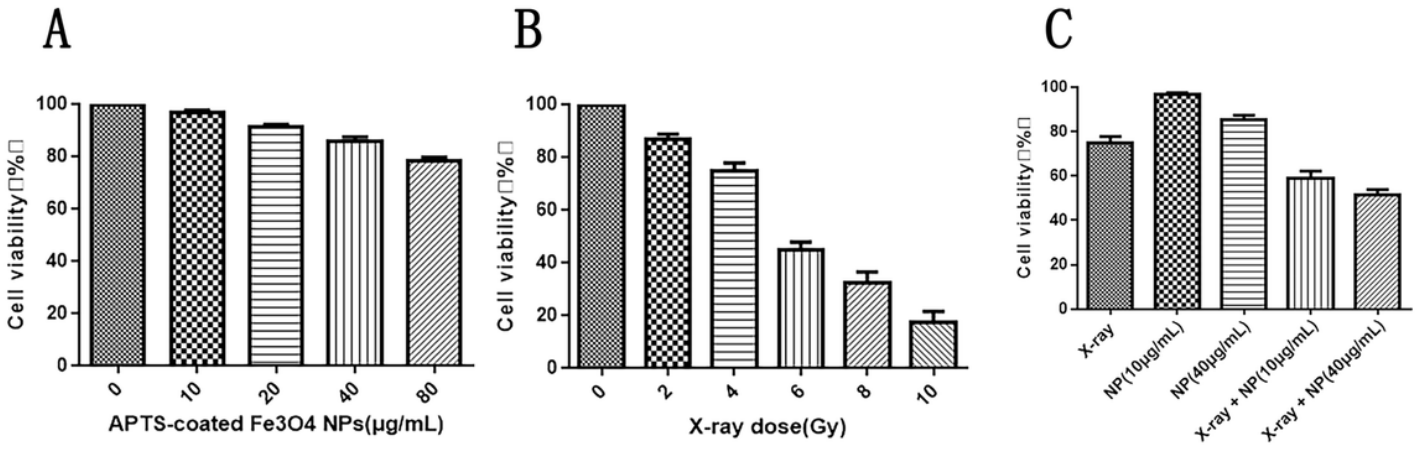

Figure 1

Characterization of acetylated APTS-coated Fe3O4 NPs. A. TEM images of NPs. B. The diameter distribution of NPs analyzed by TEM. C. The diameter distribution of NPs analyzed by DLS.

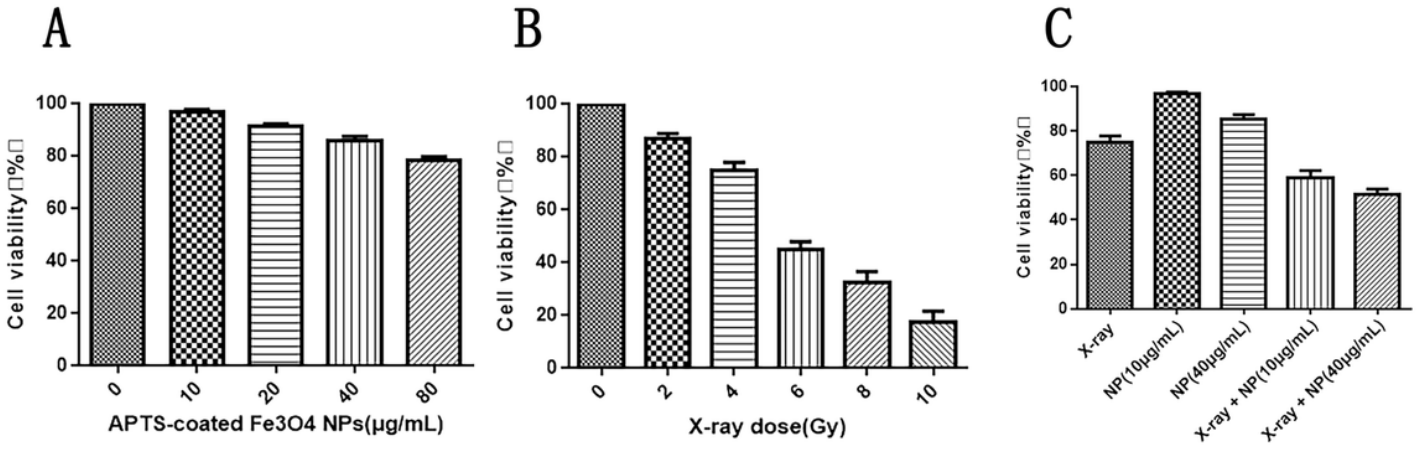

Figure 1

Characterization of acetylated APTS-coated Fe3O4 NPs. A. TEM images of NPs. B. The diameter distribution of NPs analyzed by TEM. C. The diameter distribution of NPs analyzed by DLS.

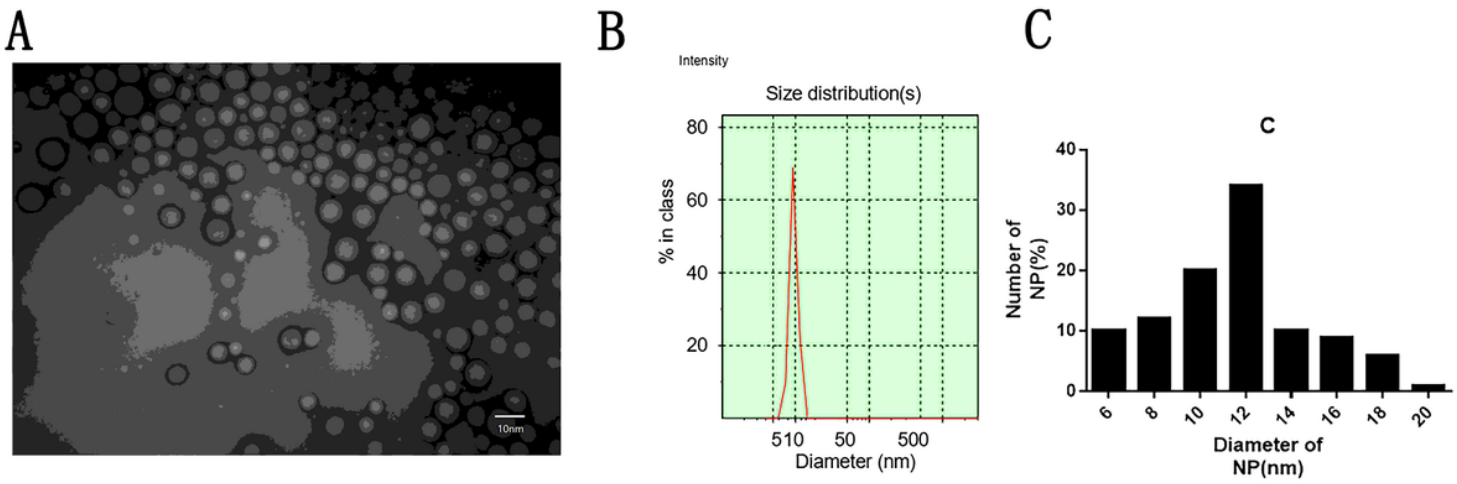

Figure 2

Intracellular uptake of NPs. A. The intracellular uptake of acetylated APTS-coated Fe3O4 NPs was quantified using ICP-AES after U87 cells were treated with NPs at different concentrations for 24 h. B. The intracellular uptake of acetylated APTS-coated Fe3O4 NPs was quantified at different time point.

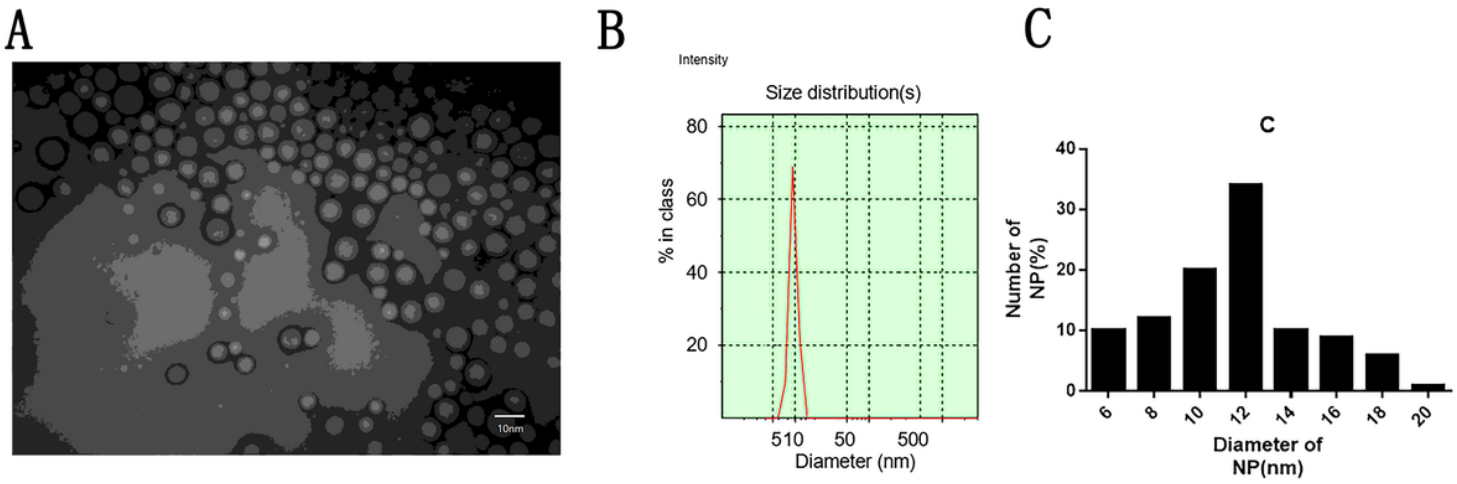

Figure 2

Intracellular uptake of NPs. A. The intracellular uptake of acetylated APTS-coated Fe3O4 NPs was quantified using ICP-AES after U87 cells were treated with NPs at different concentrations for 24 h. B. The intracellular uptake of acetylated APTS-coated Fe3O4 NPs was quantified at different time point.

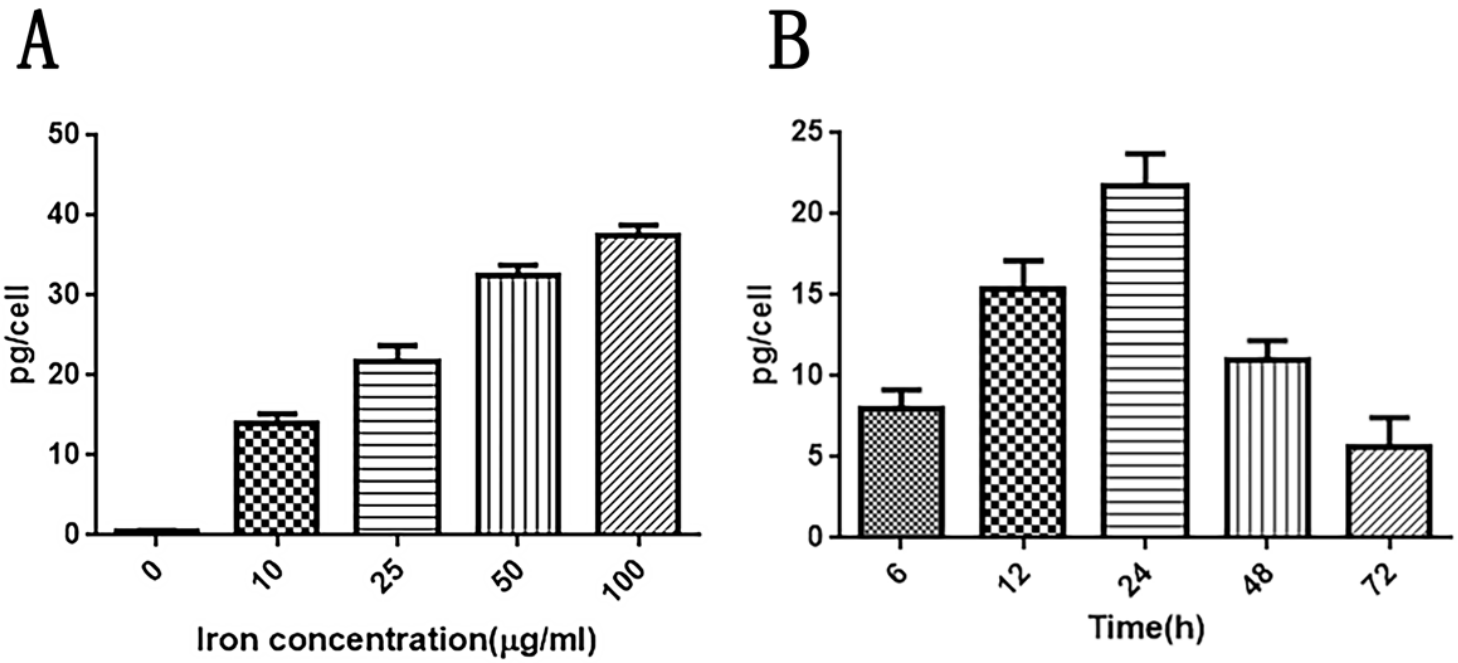

Figure 3

Cell viability tested by MTT assay. A. U87 cell viability after treatment with NPs at different concentrations. B. U87 cell viability after treatment with X-ray at different doses. *P<0.05 compared to 0 Gy. C. U87 cell viability after treatment with NPs or/and X-ray. *P<0.05 compared to X-ray alone.

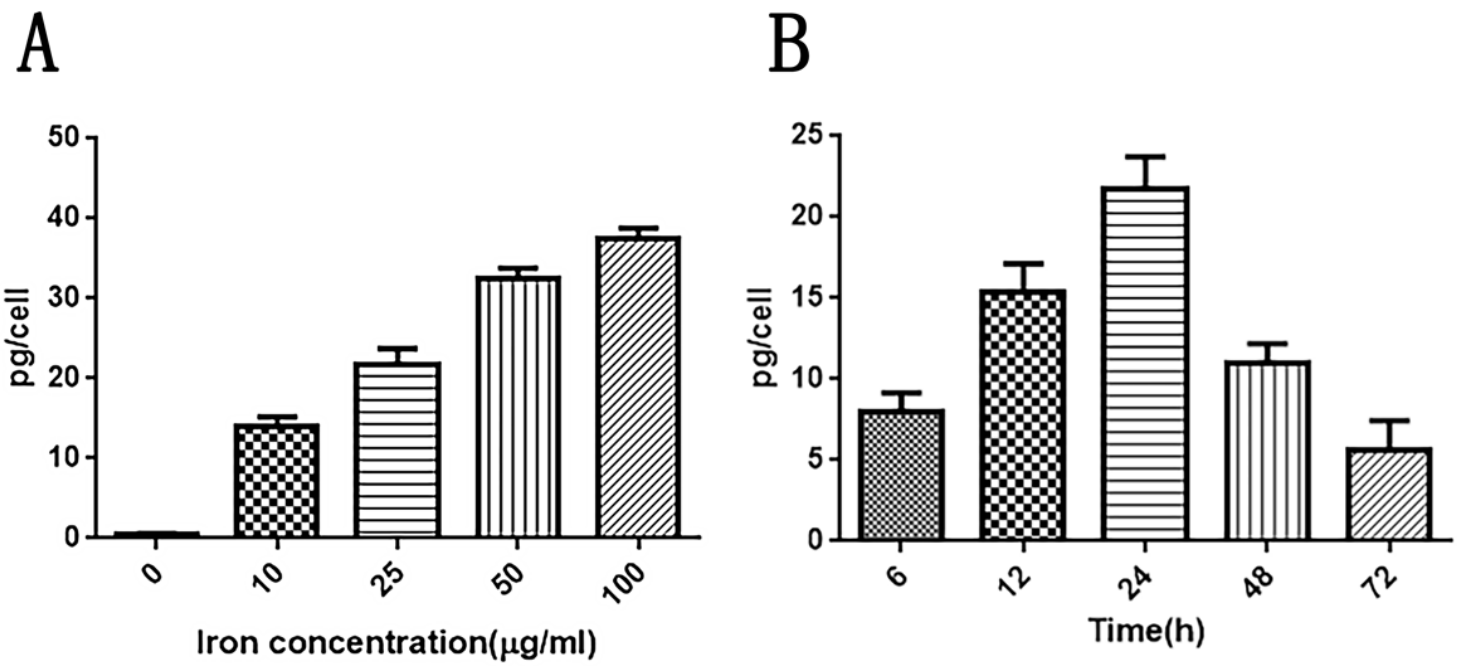

Figure 3

Cell viability tested by MTT assay. A. U87 cell viability after treatment with NPs at different concentrations. B. U87 cell viability after treatment with X-ray at different doses. *P<0.05 compared to 0 Gy. C. U87 cell viability after treatment with NPs or/and X-ray. *P<0.05 compared to X-ray alone.

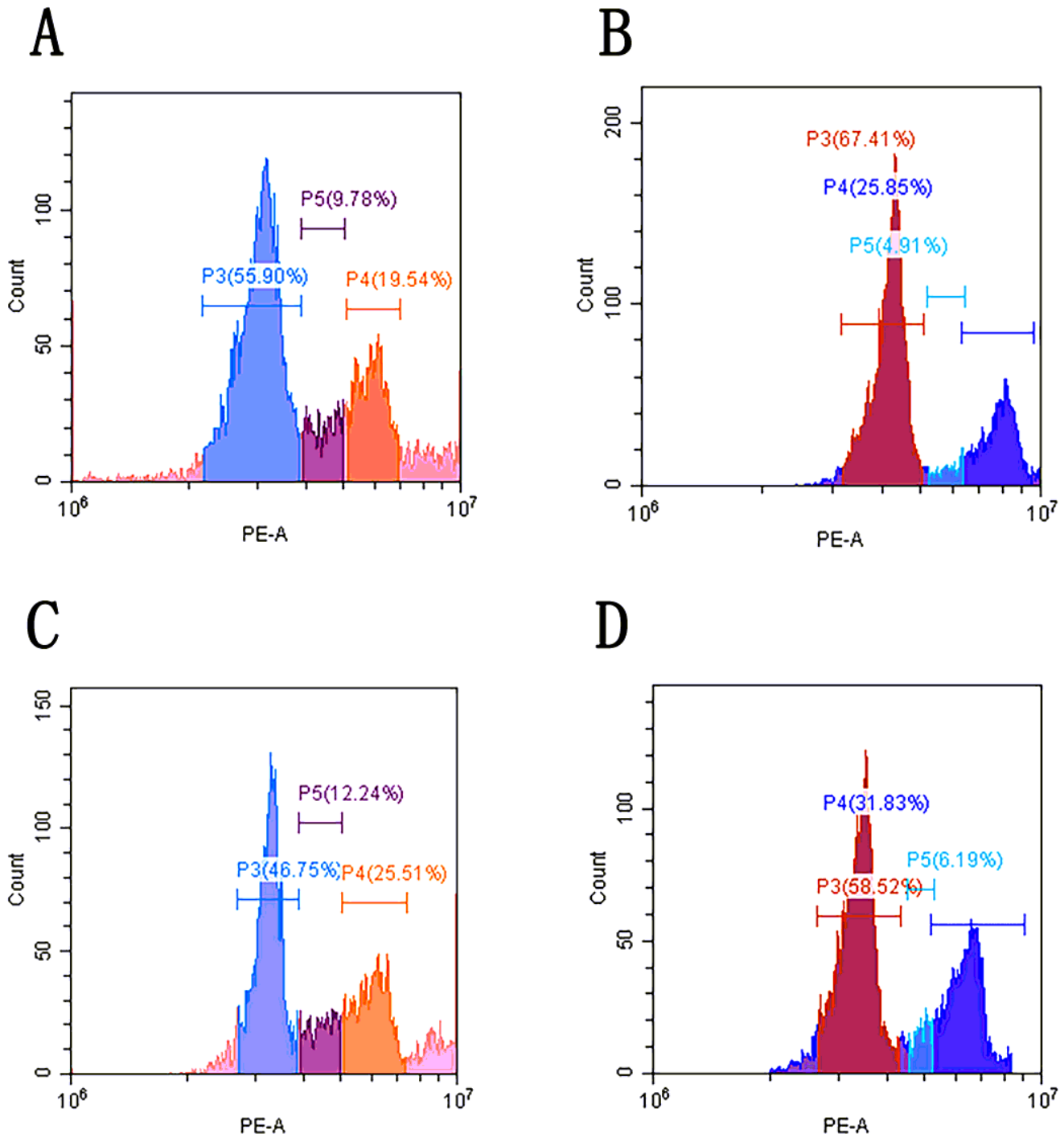

Figure 4

Flow cytometric analysis of cell cycle of U87 cells. A. Control (no treatment). B. Treatment with APTS-coated Fe3O4 NPs. C. Treatment with 4 Gy X-ray. D. Treatment with APTS-coated Fe3O4 NPs plus 4 Gy X-ray. P3: G0/G1 phase, P4: G2/M phase, P5: S phase.

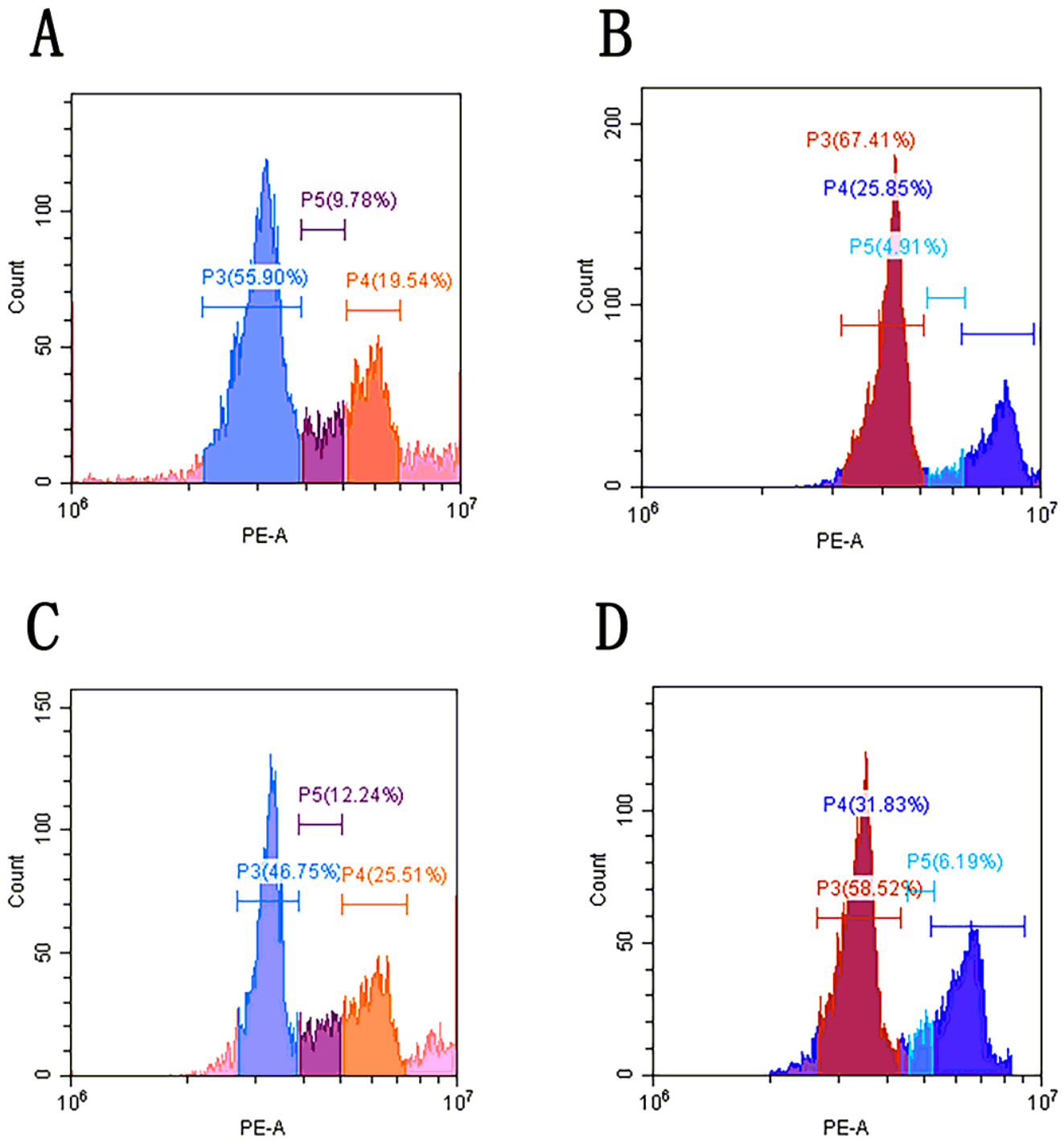

Figure 4

Flow cytometric analysis of cell cycle of U87 cells. A. Control (no treatment). B. Treatment with APTS-coated Fe3O4 NPs. C. Treatment with 4 Gy X-ray. D. Treatment with APTS-coated Fe3O4 NPs plus 4 Gy X-ray. P3: G0/G1 phase, P4: G2/M phase, P5: S phase.

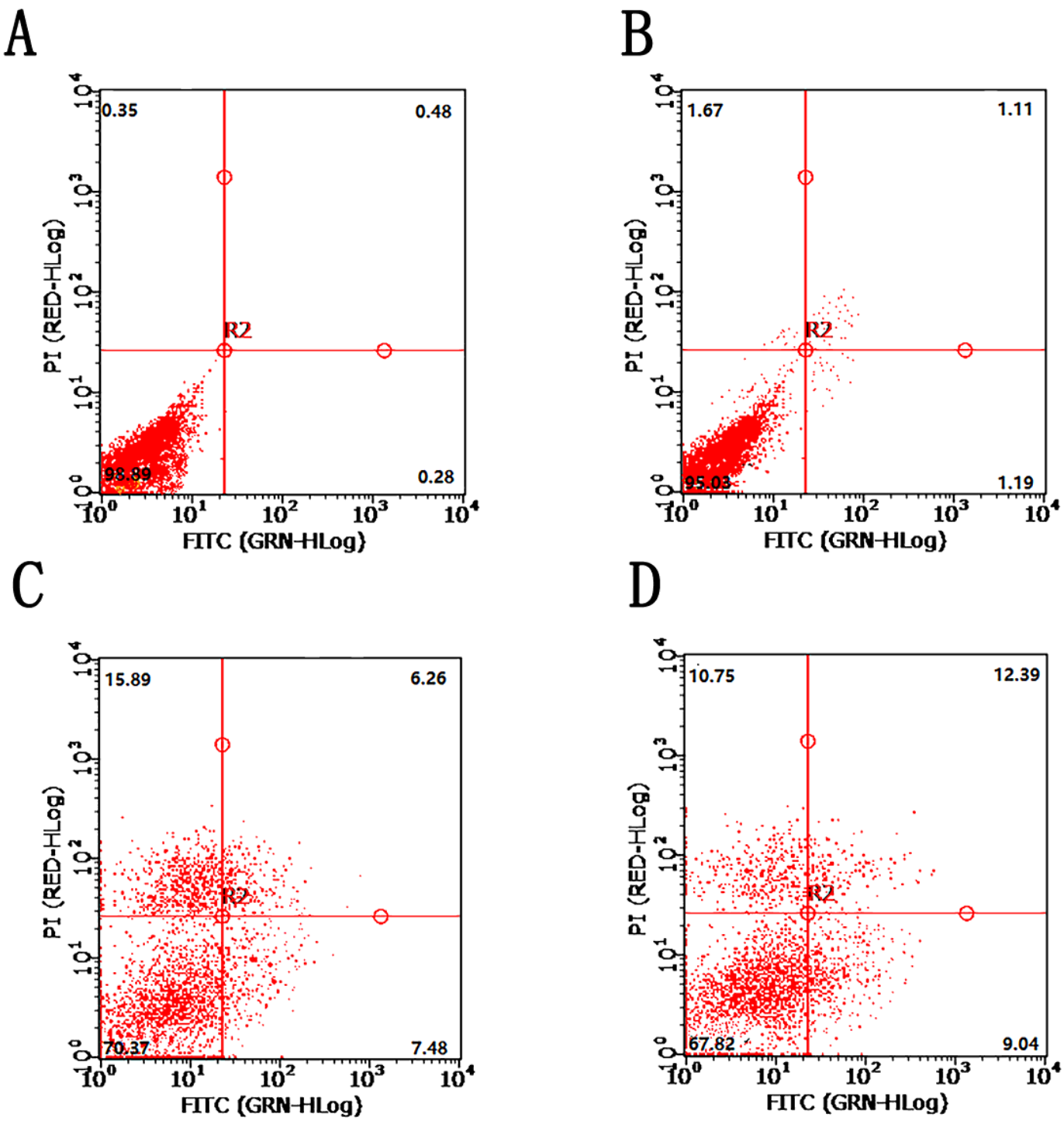

Figure 5

Scatter plots of apoptosis in different treatment groups assessed by Annexin V/PI double staining and flow cytometry. A. Control (no treatment). B. Treatment with APTS-coated Fe3O4 NPs. C. Treatment with 4 Gy X-ray. D. Treatment with APTS-coated Fe3O4 NPs plus 4 Gy X-ray.

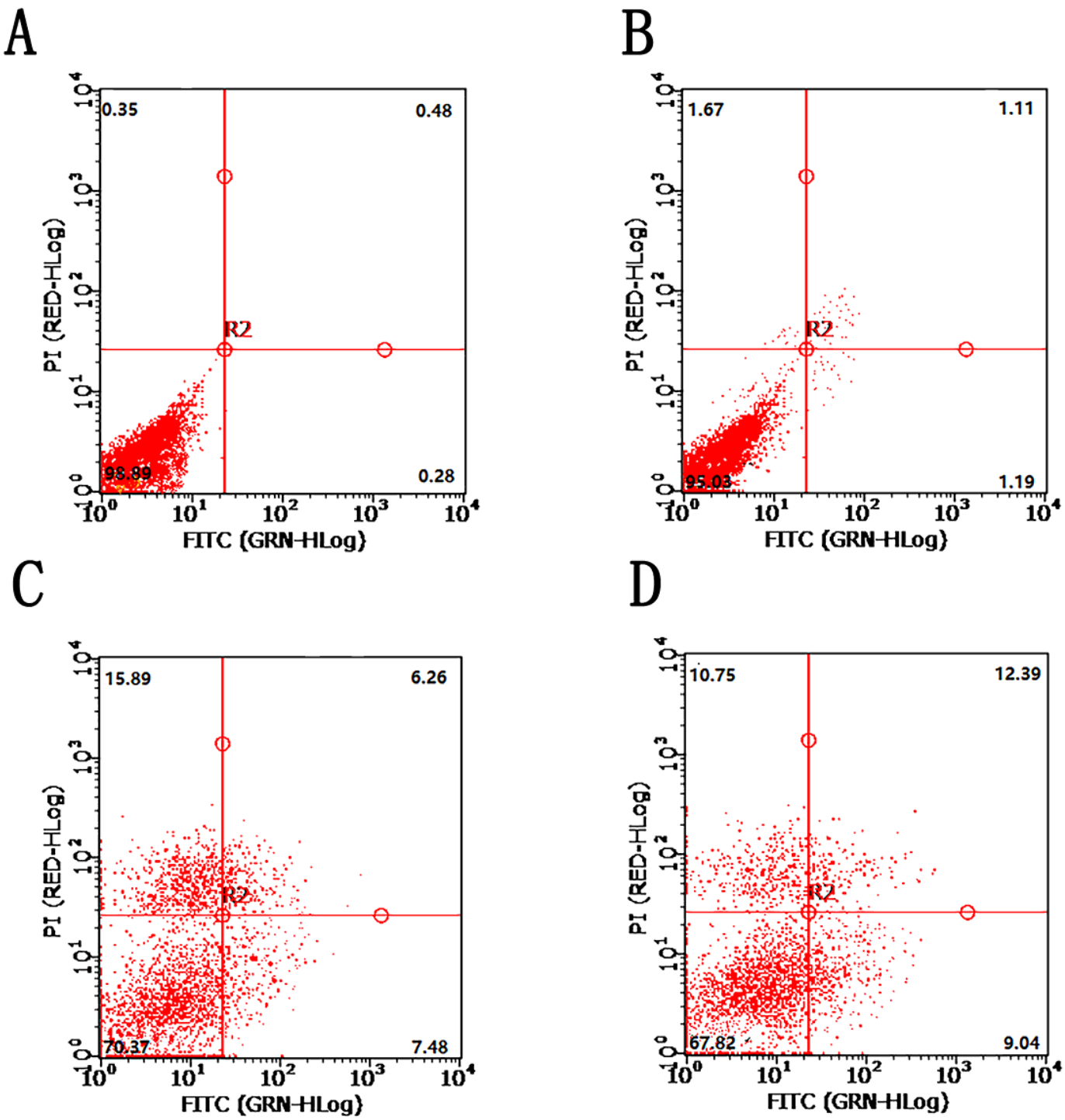

Figure 5

Scatter plots of apoptosis in different treatment groups assessed by Annexin V/PI double staining and flow cytometry. A. Control (no treatment). B. Treatment with APTS-coated Fe3O4 NPs. C. Treatment with 4 Gy X-ray. D. Treatment with APTS-coated Fe3O4 NPs plus 4 Gy X-ray.